Turk J Elec Eng & Comp Sci, Vol.20, No.Sup.1, 2012, © TÜBİTAK
doi:10.3906/elk-1102-1050

Broken rotor bar fault detection in inverter-fed squirrel cage induction motors using stator current analysis and fuzzy logic

Mehmet AKAR[1,*], **İlyas ÇANKAYA**[2]
[1]*Department of Mechatronics, Faculty of Engineering and Natural Sciences, Gaziosmanpaşa University, 60200 Tokat-TURKEY*
e-mail: mehmetakar@gop.edu.tr
[2]*Department of Electronics and Communication Engineering, Faculty of Engineering and Natural Sciences, Yıldırım Beyazıt University, Ankara-TURKEY*
e-mail: icankaya@ybu.edu.tr

Received: 17.02.2011

Abstract

This paper presents the implementation of broken rotor bar fault detection in an inverter-fed induction motor using motor current signal analysis (MCSA) and prognosis with fuzzy logic. Recently, inverter-fed induction motors have become very popular because of their adjustable speed drive. They have been used in many vital control applications such as rolling mills, variable speed compressors, pumps, and fans. The condition monitoring of these motors can significantly reduce the cost of maintenance in the early detection of faults. In this study, MCSA is applied to an inverter-fed induction motor to detect broken rotor bar faults. The diagnosis of a broken rotor bar fault in the squirrel cage induction motor, driven by an inverter, has been studied for stable, full load condition and has been carried out experimentally by analyzing the power spectrum density of the motor stator current. Motor stator currents are uploaded to a PC with the software of the inverter used and the current harmonics are obtained using LabVIEW for every fault condition. After extracting the characteristic frequencies of the broken rotor bar failure, a fuzzy logic algorithm is implemented for classifying the fault. Although there is much research on rotor bar faults for line-connected induction motors, there are no studies on the inverter-fed induction motor and fault diagnosis with fuzzy logic. The implementation results showed that the method is very efficient and useful for prognosis of the rotor faults.

Key Words: *Condition monitoring, power spectral density, rotor fault, fuzzy logic*

1. Introduction

Induction motors are the workhorses of industry and are frequently used in many applications because of their simple structure, inexpensive cost, and stability. There are 2 types of induction motors that are used in this

*Corresponding author: Department of Mechatronics, Faculty of Engineering and Natural Sciences, Gaziosmanpaşa University, 60200 Tokat-TURKEY

industry. One is the squirrel cage induction motor and the other is the wound rotor induction motor. Squirrel cage induction motors have been used frequently in industrial applications due to their low price, robustness, simple structure, and easy maintenance. Recently, inverter-fed induction motors have been increasingly used in many industrial applications such as rolling mills, variable speed compressors, pumps, and fans. The early detection of anomalies in motor drive systems is very important for safe, economic, and uninterrupted operations [1]. There are many faults that can occur in electrical machines. The percentage of failures and induction motor faults can be clearly seen in Table 1 and Figure 1 [2].

Table 1. Percentage of failures [2].

	IEEE-IAS (%) Electrical Safety Workshop 1985a	IEEE-IAS (%) Electrical Safety Workshop 1985b	EPRI (%) Electric Power Research Institute 1985c
Number of faulty motor	380	304	1052
Bearing-related	44	50	41
Winding-related	26	25	36
Rotor-related	8	9	9
Other	22	26	14

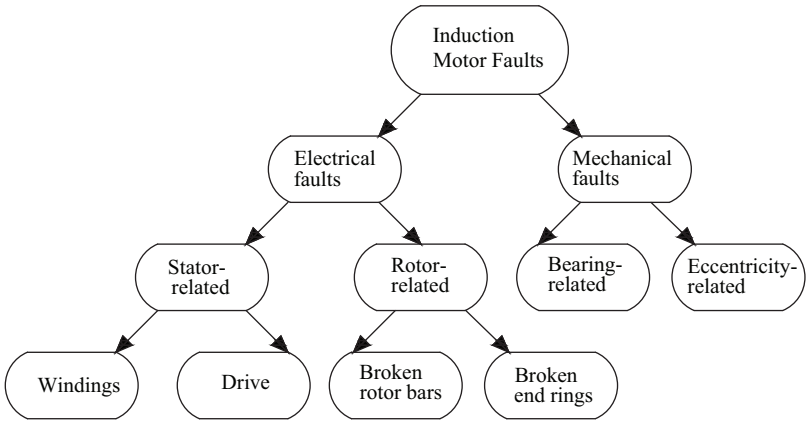

Figure 1. Induction motor fault scheme [2].

These induction motor faults can be classified as stator faults, resulting from opening or shorting one or more of the stator phases, incorrect connection of the motor windings, broken or cracked rotor bars or end rings, motor air-gap irregularities, and bearing or gearbox failures [3]. All of the above faults cause symptoms such as unbalanced air-gap voltages and motor currents stemming from an unbalanced magnetic pull, load torque oscillation, reduced average motor torque, increased losses with decreased motor efficiency, and increased motor temperature [3].

The remainder of this paper is organized as following: Section 2 describes the literature survey on broken rotor bar faults. Sections 3 and 4 explain the signal analysis method, power spectrum density (PSD), and the proposed fault diagnosis algorithm, respectively. The experimental study and the numerical results are analyzed in Section 5. Finally, the paper concludes in Section 6.

2. Broken rotor bar faults

Squirrel cage rotor design and manufacturing have undergone little change over the years [4]. Rotor-related faults are usually associated with thermal stresses, magnetic stresses from electromagnetic forces, residual stresses in insufficient manufacturing, and environmental stresses that are caused by moisture [3]. Rotor faults start at high resistance, causing high temperatures, and then progress as cracking or small holes in the rotor bars [5]. These faults are more likely to take place at the cage end rings. Different motor parameters such as pulsations in speed, air gap flux, vibration, and motor current signature can be monitored for the detection of broken rotor bars. Early fault detection techniques, which are designed for these motors, can significantly reduce maintenance costs. Thus, condition monitoring studies aim at fault diagnosis in electric motors. In this sense, the spectral analysis methods are regarded as one of the outstanding techniques in the literature [6-10].

Although this method needs extra sensors, there is no problem in using the motor current signal analysis (MCSA) method, because the inverter fed-induction motor drive includes current, voltage, and speed sensors. This method provides a highly sensitive, selective, and cost-effective meaning for online monitoring of heavy industrial machinery. Spectrum analysis has been the preference of most researchers. Thomson and Stewart [11], Kliman et al. [12], Flippetti et al. [13], and Elkasabgy [14] used the MCSA spectrum to detect broken bar faults. They demonstrated sideband components f_b around the fundamental frequency to detect broken bar faults. The lower sideband is specific to a broken bar, while the upper sideband is a consequence of speed oscillation. f_0 is the frequency of the supply phase current, s is the motor slip, and $k = 0, 1, 2, \ldots, n$.

$$f_b = (1 \pm 2ks) f_0 \tag{1}$$

The magnitude of the sideband components changes in accordance with the load inertia. In addition to Eq. (1), other spectral components that occur can be observed in the motor line current with the aid of the equation below [15].

$$f_b = \left(\frac{k}{p}\right)(1 - s) \pm s) f_0 \tag{2}$$

p denotes the number of pole pairs ($p = 2, 4, \ldots, n$). Figure 2 shows the frequency of specific components for a broken rotor bar fault, which is given in Eq. (1) for $k = 1$ and 2. These frequencies are located around the fundamental line frequency and are called the lower sideband and upper sideband components, as indicated in Figure 2 [16].

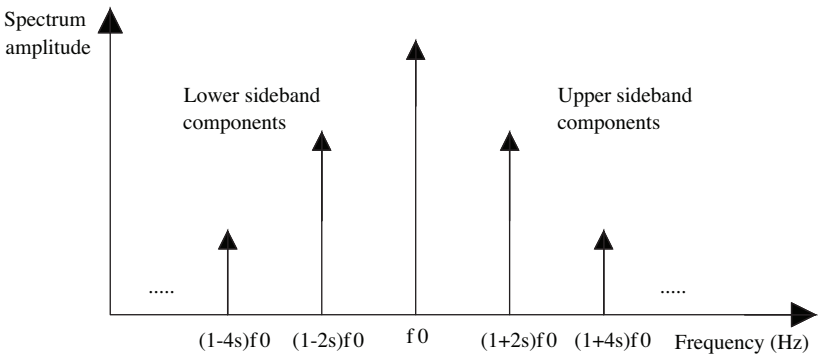

Figure 2. Fundamental and sideband frequencies [15].

Çalış and Çakır experimentally studied sensorless broken bar detection [5]. Their experimental results showed that sensorless broken bar detection in induction motors based on fluctuations of the stator current zero-crossing instants was very efficient before actual breakdown occurred. They used a microcontroller to determine these fluctuations, and the fast Fourier transformation (FFT) algorithm was used to monitor the amplitude changes on specific frequency components. Cho et al. used state and parameter estimation techniques for broken rotor bar diagnosis [17]. Masoud and Toliyat estimated the rotor speed on the basis of the stator current; then the featured vector was extracted as an input to the Bayes classifier and they used the pattern recognition technique to detect broken rotor bars [15].

3. Power spectral density

The Fourier transform (FT) defines a relationship between a signal in the time domain and its representation in the frequency domain. According to the FT, which was first used in 1807 by Joseph Fourier, all of the continuous functions with a fundamental period of $T_0(w_0 = 2\pi/T_0)$ can be expressed by the trigonometric functions [18]. Although the FT was successfully used for stationary signals, it was insufficient for nonstationary signals because of the missing time data. This problem was noticed by Denis Gabor while he was using short-time Fourier transform (STFT) in 1946. The STFT is an approach that can give information on the time resolution of the spectrum. The STFT analyzes the time signal by windowing, so it is also called the windowed FT. The STFT uses different types of windowing functions, such as '*hanning*', '*hamming*', '*chebyshev*', or '*kaiser*'. The STFT applications in engineering are limited because of its fixed window, which results in low time-frequency resolution.

Recently, the FFT has been used efficiently for signal processing applications such as motor current signal analysis and digital signal processing. The FFT is also a useful method for calculating the discrete Fourier transform. Even though it produces the same result as the other approaches, it is incredibly more efficient and reduces the computation time. This method operates by decomposing the N-point time-domain signal into N time-domain signals, each composed of a single point. The second step is to calculate the N frequency spectra corresponding to these N time-domain signals. Finally, the N spectra are synthesized into a single frequency spectrum [19].

The PSD is the estimation of the spectrum of discrete-time deterministic and stochastic processes and it has generally been used for useful signal processing techniques. PSD processes simply find the discrete-time FT of the collected signals to obtain the magnitude of the results. The PSD expresses the amount of the power density of the spectrum as a function of the frequency, and it describes how the power of a time series is distributed with frequency. With the help of the knowledge of the PSD and system bandwidth, the total power can be calculated. The FFT can convert time-domain signals $ws_i(n)$ into the frequency domain:

$$ws_i(f) = \frac{1}{M}\sum_{n=0}^{M-1} ws_i(n)e^{-j2\pi n\frac{f}{m}} \quad . \tag{3}$$

$f = 0, 1, 2, \ldots N$ where f is discrete frequency, and the raw power spectral estimate can be calculated as:

$$PSD_i(f) = \frac{1}{M} ws_i(f)\,\mathrm{xws_i^*}(f), \tag{4}$$

where * denotes the complex conjugate. Moreover, raw PSD estimates from all of the segments can be averaged

to give the following equation:

$$PSD_i(f) = \frac{1}{k}\sum_{i=0}^{k-1} PSD_i(f). \tag{5}$$

4. Fuzzy logic-based fault diagnosis

Recently, artificial intelligence (AI) has been used in many applications, such as electrical motor controls, robotics, fault diagnosis, etc. One type of AI model is the fuzzy model, which defines its input and output as attributive values and then defines the strength of the relationships between these input and output reference sets [20]. This capability provides a useful method for analyzing the motor current and establishing the faults. In recent research, the condition monitoring and fault detection of electrical motors have moved to AI techniques, including neural networks and fuzzy logic, from traditional methods, because no detailed analysis of the fault mechanism is necessary and no modeling is required [21].

There are many studies on motor fault identification with fuzzy logic and artificial neural networks (ANNs). Serial wound direct current motor faults are investigated with multilayer feedforward neural network structures, such as neural network fault diagnosis (NNFD) [22]. NNFD was trained using the backpropagation algorithm. In addition, those authors studied fuzzy logic-based fault diagnosis on serial wound motors [23]. They measured voltage and current signals and they decomposed signal components by using wavelet analysis. Wavelet coefficients were classified using fuzzy logic. Pereira and Silva studied the practical implementation of a system for the detection and diagnosis of broken rotor bars in electrical induction motors [24]. Goddu et al. analyzed bearing vibration signals using fuzzy logic fault diagnosis methodology [25]. Their study results showed that fuzzy logic can be used for accurate bearing fault diagnosis if the input data are processed in an advantageous way.

5. Application

In this study, a 1.1-kW, 2-pole delta connected squirrel cage induction motor (AGME 802b) was used, with parameters given in Table 2. The motor is loaded with an eddy current brake, whose armature voltage and current are 48 V DC and 2.2 A, respectively. The squirrel cage induction motor was driven by a Siemens Sinamics CU 310 DP inverter.

Table 2. Rated parameters of the tested machine.

Power	1.1	kW
Frequency	50	Hz
Voltage (Δ/Υ)	220/380	V
Current (Δ/Υ)	4.04/2.34	A
Speed	2900	rpm
Power factor	0.82	
Pole pair (2p)	2	

The purpose of the motor monitoring system was to measure the motor stator current. The measured current data were uploaded to a PC with the software of the inverter used, and then the current harmonics

were obtained using LabVIEW. The motor current data were acquired at a 2-kHz sampling rate under different load conditions. The motor test bench and broken rotor bars are illustrated in Figures 3 and 4, respectively.

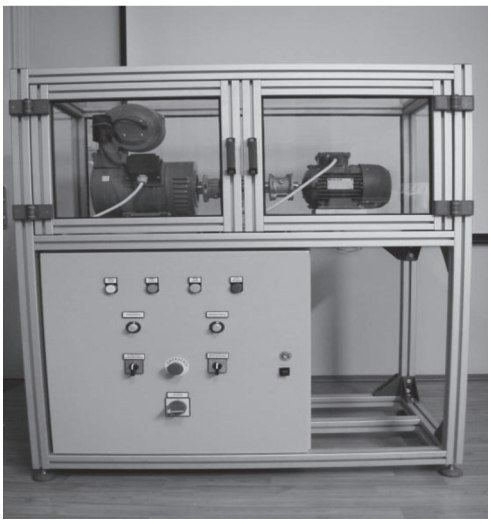

Figure 3. Motor test bench.

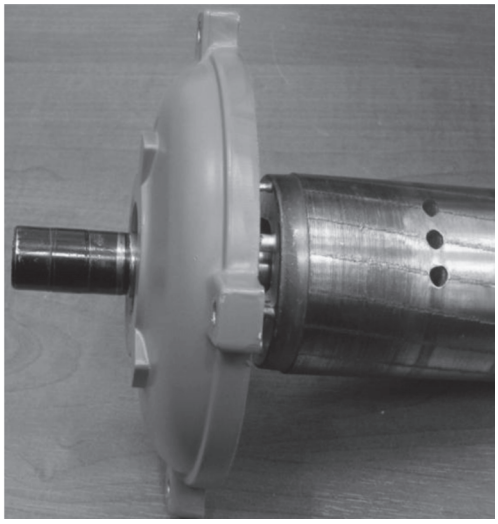

Figure 4. Rotor with 3 broken bar faults.

First, the motor was operated at 2970 rpm (s = 0.01) at no load condition, and then at 2900 rpm (s = 0.033) at a healthy full load condition; motor current was acquired during 60 s (120,000 data points with 2000/120,000 = 0.016 Hz resolution). After this, the motor rotor bars were artificially broken by drilling a 6-mm hole for 1, 2, and 3 broken bar faults and a 3-mm hole for 1 or 2 and 2 or 3 broken bar faults. Although these were not realistic rotor bar failures, the artificial faults produced characteristic fault frequencies. With 1 broken rotor bar fault motor current measured under no-load and full-load conditions, this process was repeated with 3 broken rotor bars. When the motor current data were investigated in the time domain, their healthy and faulty situations were nearly the same, which is illustrated in Figure 5.

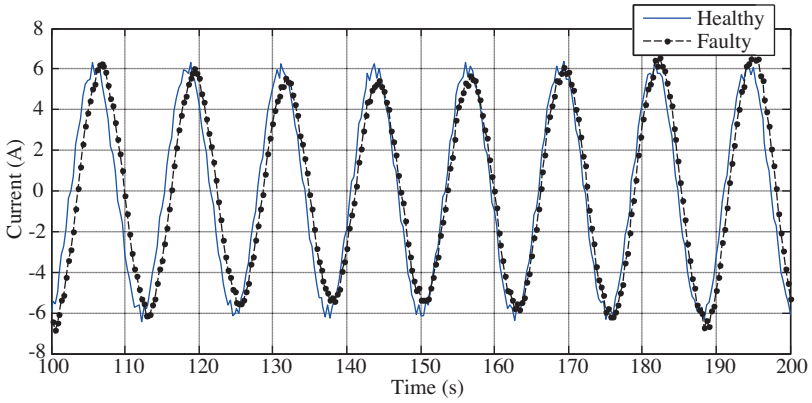

Figure 5. Full-load motor current with 3 broken bars.

For extracting the broken bar characteristic frequencies, the PSD transform was applied to the time-domain signal using LabVIEW. While PSD was applied, the Welch method and Hanning window were used. The results show that when the rotor was healthy, there were no sidebands around the fundamental frequency. With rotor broken bar faults, the lower and upper sideband components occurred around the fundamental

frequency. The sideband component amplitude depends on the number of broken bars and their place depends on the motor slip. The current spectra of the healthy and the faulty motor under no-load conditions are shown in Figures 6a-6d.

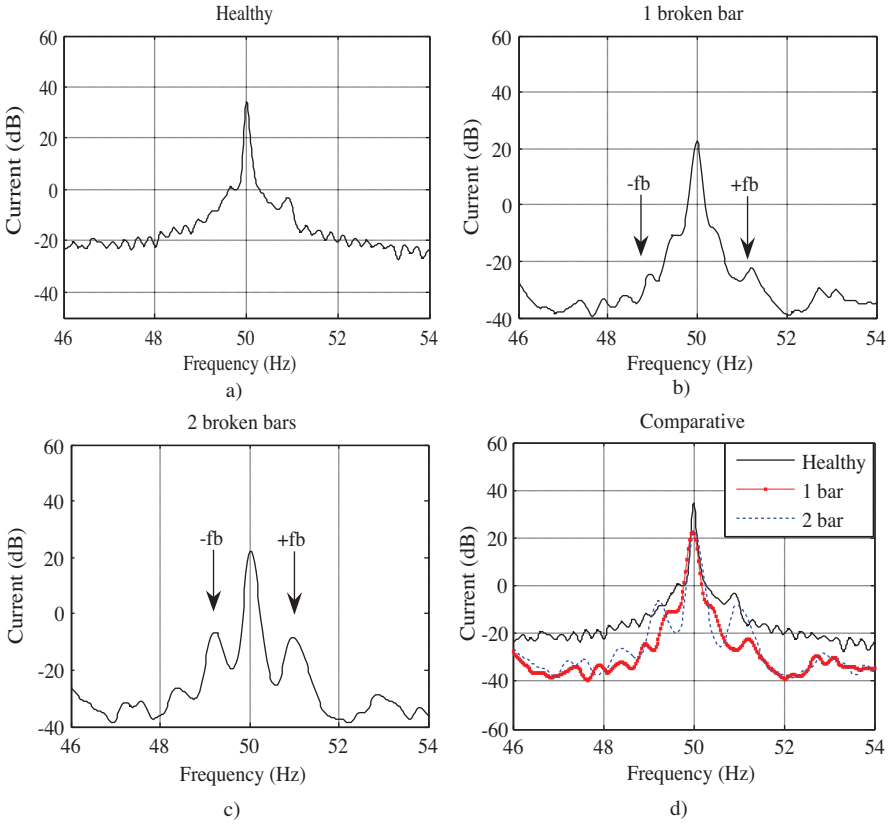

Figure 6. Motor current spectra under no-load conditions.

With broken bar faults, the lower and upper sideband components occurred at 49 Hz $(-f_b = (1-2ks)f_0)$ and at 51 Hz $(+f_b = (1+2ks)\,f_0)$, depending on $k = 1$ and the motor slip (s = 0.01). When the broken bar number was increased, the sideband component amplitude changed in accordance with the number of broken bars. In Figure 6d, a comparative study is shown with different broken bars. While the motor was operating at no-load conditions, it was also difficult to find the sideband components because of the lower amplitude and closeness to the fundamental frequency. Under the full-load conditions, the motor slip increased at s = 0.033 and the sideband components left the fundamental frequency. In Figure 7, current spectra of the motor full-load conditions are illustrated.

Under full-load conditions, the lower sideband component occurred at 46.7 Hz $(-f_b = (1-2ks)f_0)$ and the upper side band component occurred at 53.3 Hz $(+f_b = (1+2ks)\,f_0)$. In Figure 8, it is shown that not only has the characteristic frequency occurred around the fundamental frequency, but it has also occurred at the 3rd and 5th harmonics of fundamental frequency.

In order to see broken bar effects on the motor current spectrum at a low speed, the motor was operated at a 30-Hz supply frequency. While the motor was operating at 30 Hz, the motor current was acquired for no load and full load with 2 broken bar faults existing. It is seen that the same symptoms are clearly presented in the spectrum graph (Figure 9).

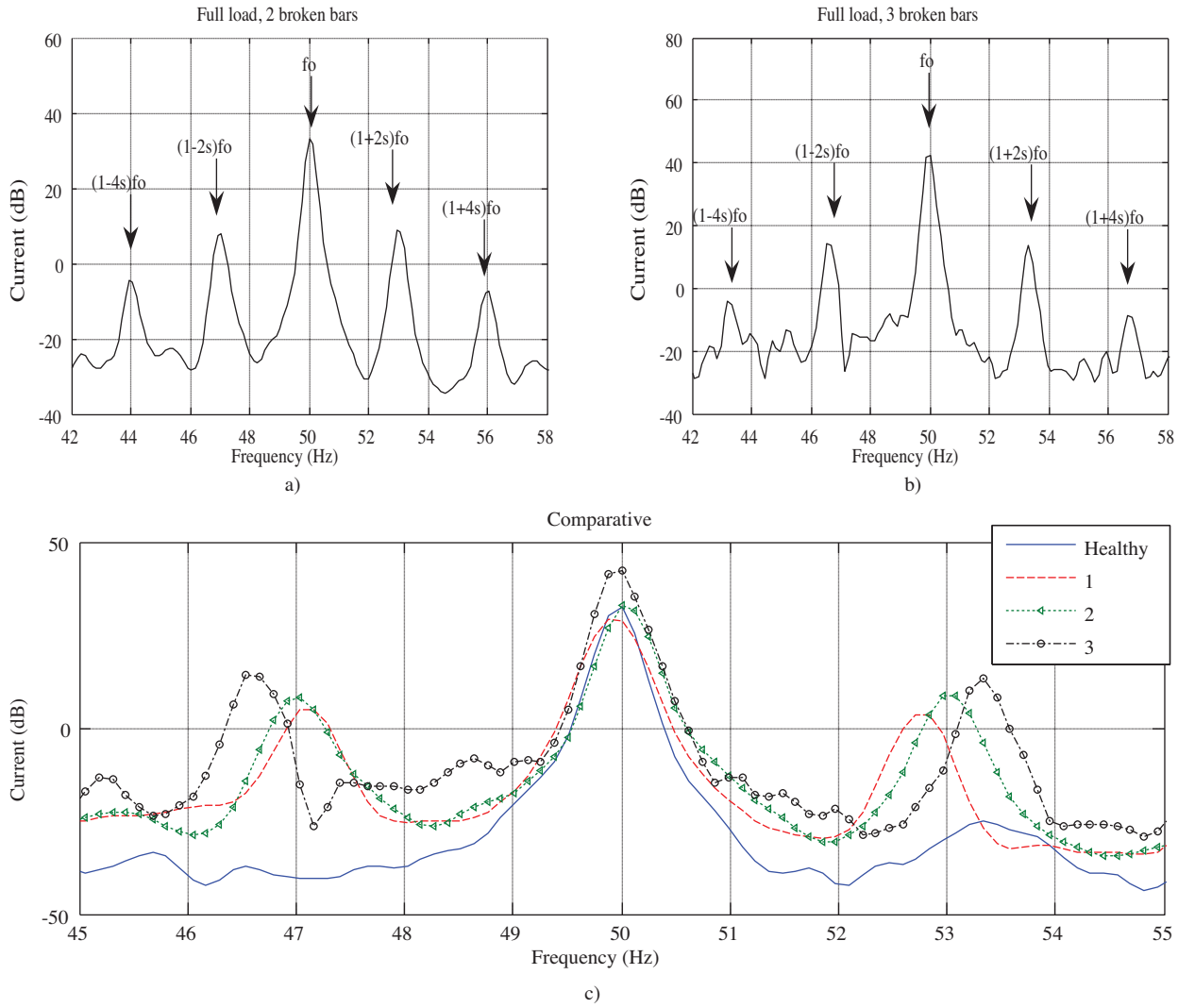

Figure 7. Motor current spectra under full-load conditions.

There are 2 spectrum components that increase when the number of broken bars increases. The amplitudes of these spectrum components are dependent on different parameters, such as load, inertia, and speed ripple. However, in general, the amplitudes of these components increase when the number of broken rotor bars increases [26]. The amplitudes of these components, referred to as the amplitudes of the fundamental component in dB, are denoted by the lower sideband (LS) and upper sideband (US), respectively [26]. By using LS and US as the inputs of a fuzzy logic-based diagnostic system, it is possible to detect the presence of broken rotor bars in a squirrel cage induction motor, and it is also possible to determine the specific number of broken rotor bars (Figures 10a-10f). The fuzzy logic-based broken rotor bar prognosis system, described below, has 2 inputs (LS and US) and a single output, and it is based on the expert rules, which give the connection of LS, US, and the number of broken bars (n) [26]. In a real system, it is possible to use a relatively small number of rules. According to this, a diagnostic system must also detect the threshold between healthy and faulty conditions, and it must also eliminate the speed and load torque ripple. Therefore, as a result, 7 conditions are considered: no broken bars (NO), incipient fault (IF), 1 broken bar (O), 1 or 2 broken bars (O-T), 2 broken bars

(T), 2 or 3 broken bars (T-T), and 3 broken bars (TH). The linguistic values defined for the input set are small (S), medium (M), large (L), and very large (VL). The centroid method was used for defuzzification because it produces the best results. Many types of membership functions were simulated and bell-shaped functions were chosen because they give the best error results. Sixteen rules were used to detect the various rotor faults, as given in Table 3.

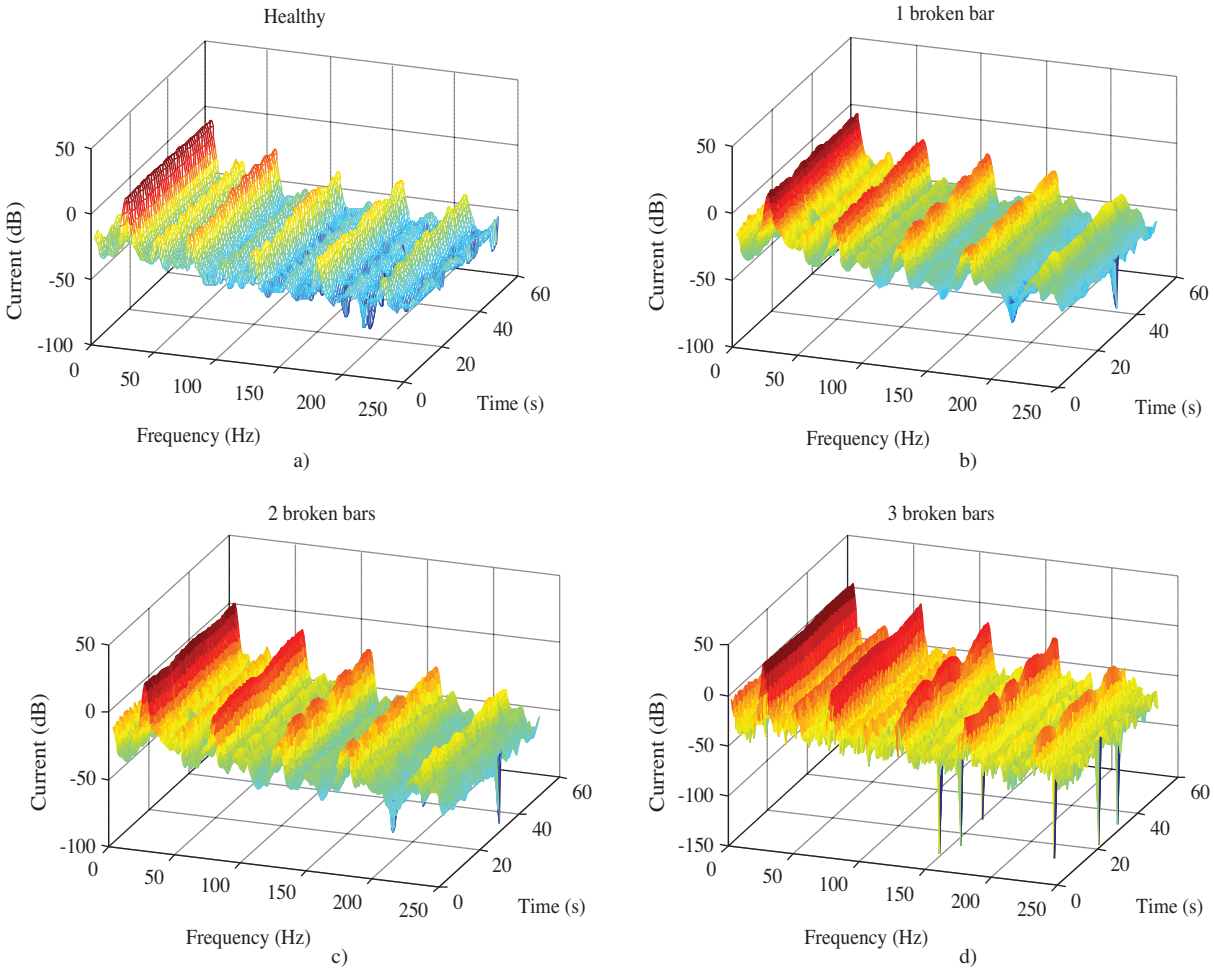

Figure 8. Full-load motor current surfaces with a different number of broken bars.

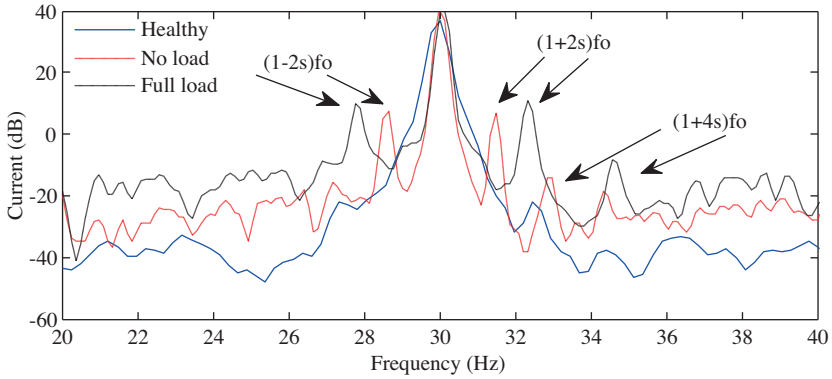

Figure 9. Motor current spectra under no- and full-load conditions (30 Hz).

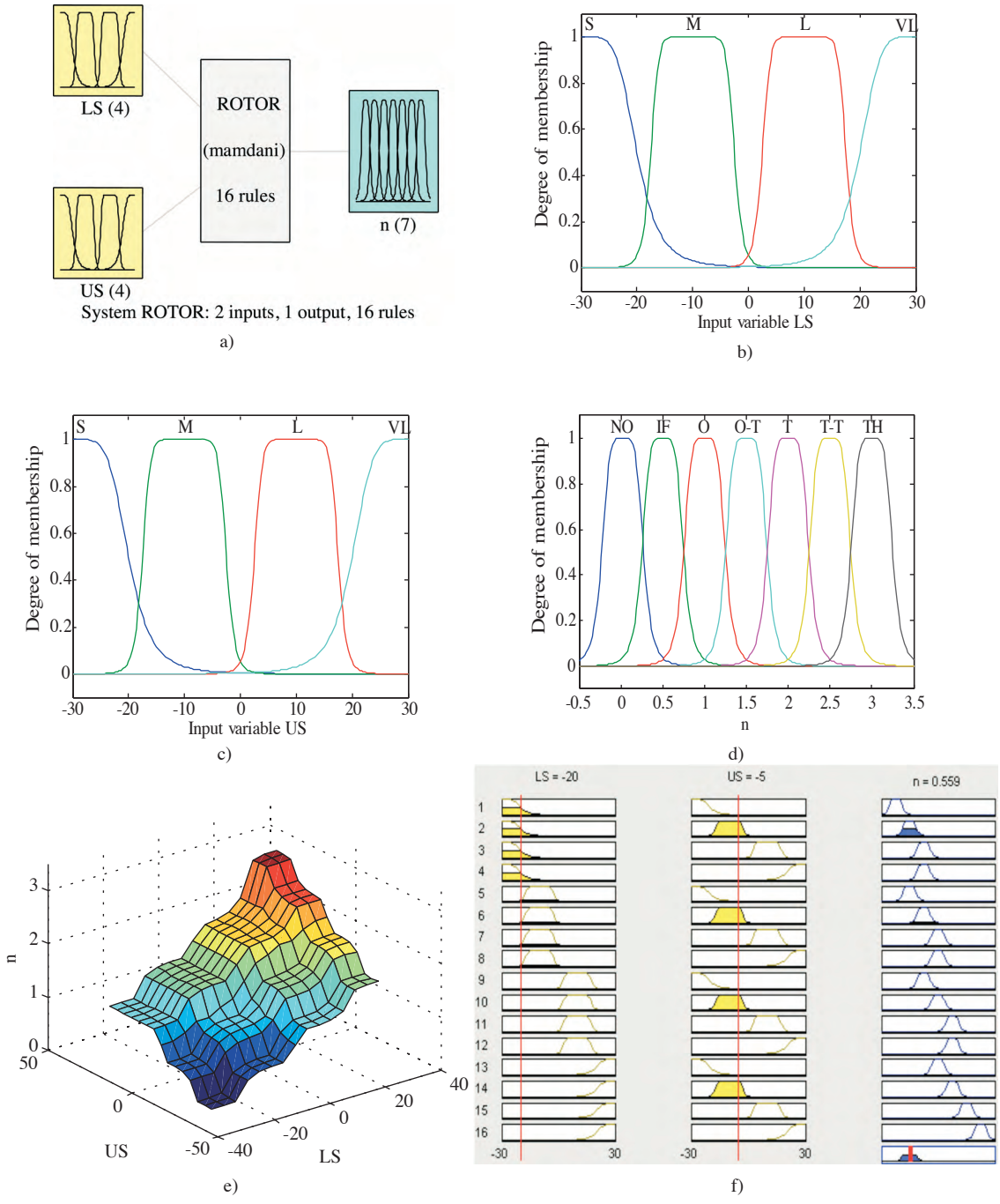

Figure 10. a) Fuzzy-based system, b) input membership functions for LS, c) input membership functions for US, d) output membership functions for n, e) surface plot, and f) rule view.

The fuzzy logic-based fault diagnostic system was tested and applied in the experimental study. For example, the LS = –20 dB and US = –5 dB output value of 0.559 was obtained, which corresponds to the incipient fault illustrated in Figure 10f. The LS = 0 dB and US = 5 dB output value of 1.74 was also obtained, which was due to 1 or 2 broken bars.

Table 3. Input-output relationship rules.

1. If (LS is S) and (US is S) then (n is NO)	9. If (LS is L) and (US is S) then (n is O)
2. If (LS is S) and (US is M) then (n is IF)	10. If (LS is L) and (US is M) then (n is O-T)
3. If (LS is S) and (US is L) then (n is O)	11. If (LS is L) and (US is L) then (n is T)
4. If (LS is S) and (US is VL) then (n is O)	12. If (LS is L) and (US is VL) then (n is T)
5. If (LS is M) and (US is S) then (n is IF)	13. If (LS is VL) and (US is S) then (n is O-T)
6. If (LS is M) and (US is M) then (n is O)	14. If (LS is VL) and (US is M) then (n is T)
7. If (LS is M) and (US is L) then (n is O-T)	15. If (LS is VL) and (US is L) then (n is T-T)
8. If (LS is M) and (US is VL) then (n is O-T)	16. If (LS is VL) and (US is VL) then (n is TH)

6. Conclusions

This study investigated the implementation of detecting broken rotor bar faults using the PSD of a single-phase stator current of a squirrel cage induction motor, and the motor condition was established with the help of spectrum results. In an induction motor with rotor asymmetry, multiple spectrum harmonics appeared in the stator current due to rotor asymmetry. Thus, spectrum harmonics at $\pm f_b = (1 \pm 2ks)\, f_0$ were also presented, which can be used in rotor asymmetry. Experimental results show that while the motor was operating under no-load conditions with broken bar faults, the lower and upper sideband components occurred at 49 and 51 Hz, respectively. It was difficult to define while the motor was operating under no-load conditions because of a lower amplitude and closeness to the fundamental frequency. When the motor operated under full load conditions, the sideband components clearly occurred at 46.7 and 53.3 Hz. When the number of broken bars increased, the sideband components occurred around the fundamental and its harmonics. This situation can also be understood with the motor's full load current surface. Moreover, the amplitudes increased in accordance with the number of broken bars. The amplitudes of the harmonic components were used as inputs of the fuzzy logic-based diagnostic system. The experimental results clearly illustrate that the fuzzy logic-based system is very effective and capable of detecting the correct number of broken rotor bars. In the fuzzy logic-based system, it is necessary to know the membership functions, and the optimum membership functions have been obtained with the help of trial and error. However, it is also possible to use the fuzzy neural system, because automatically obtaining the membership function tuning is an advantage and the rules are also obtained automatically. In future studies, researchers may repeat this study to find an acceptable level of threshold to guarantee the detection sensitivity for different motor sizes and different broken bars.

References

[1] M. Akar, S. Taşkın, S. Şeker, İ. Çankaya, "Detection of static eccentricity for permanent magnet synchronous motors using the coherence analysis", Turkish Journal of Electrical Engineering & Computer Sciences, Vol. 18, pp. 963-974, 2010.

[2] C. Yeh, A. Sayed, R. Povinelli, "A reconfigurable motor for experimental emulation of stator winding inter-turn and broken bar faults in polyphase induction machines", IEEE Transactions on Energy Conversion, Vol. 23, pp. 1005-1014, 2008.

[3] S. Nandi, H.A. Toliyat, X. Li, "Condition monitoring and fault diagnosis of electrical motors - a review", IEEE Transactions on Energy Conversion, Vol. 20, pp. 719-729, 2005.

[4] N. Mehala, R. Dahiya, "Rotor faults detection in induction motor by wavelet analysis", International Journal of Engineering Science and Technology, Vol. 1, pp. 90-99, 2009.

[5] H. Çalış, A. Çakır, "Rotor bar fault diagnosis in three phase induction motors by monitoring fluctuations of motor current zero crossing instants", Electric Power System Research, Vol. 85, pp. 385-392, 2006.

[6] S. Seker, "Determination of air-gap eccentricity in electric motors using coherence analysis", IEEE Power Engineering Review, Vol. 20, pp.48-50, 2000.

[7] S. Şeker, E. Ayaz, "A reliability model for induction motor ball bearing degradation", Electric Power Components & Systems, Vol. 31, pp. 639-52, 2003.

[8] E. Ayaz, A. Öztürk, S. Şeker, "Continuous wavelet transform for bearing damage detection in electric motors", IEEE Mediterranean Electrotechnical Conference, pp. 1130-33, 2006.

[9] E. Ayaz, A. Öztürk, S. Seker, B.R. Upadhyaya, "Fault detection based on continuous wavelet transform and sensor fusion in electric motors", COMPEL: The International Journal for Computation and Mathematics in Electrical and Electronic Engineering, Vol. 28, pp. 454-470, 2009.

[10] S. Seker, E. Ayaz, "Feature extraction related to bearing damage in electric motors by wavelet analysis", Journal of the Franklin Institute, Vol. 340, pp. 125-134, 2003.

[11] W.T. Thomson, I.D. Stewart, "Online current monitoring for fault diagnosis in inverter fed induction motors", Third International Conference on Power Electronics and Variable-Speed Drives, pp. 432-435, 1988.

[12] G.B. Kliman, R.A. Koegl, J. Stein, R.D. Endicott, M.W. Madden, "Noninvasive detection of broken rotor bars in operating induction motors", IEEE Transactions on Energy Conversion, Vol. 3, pp. 873-879, 1988.

[13] F. Filippetti, G. Franceschini, C. Tassoni, P. Vas, "AI techniques in induction machines diagnosis including the speed ripple effect", IEEE Industry Applications Society Annual Meeting Conference, pp. 655-662, 1996.

[14] N.M. Elkasabgy, A.R. Eastham, G.E. Dawson, "Detection of broken bars in the cage rotor on an induction machine", IEEE Transactions on Industry Applications, Vol. 22, pp. 165-171, 1992.

[15] M. Haji, H.A. Toliyat, "Pattern recognition - a technique for induction machines rotor broken bar detection", IEEE Transactions on Energy Conversion, Vol. 16, pp. 312-317, 2001.

[16] B. Ayhan, J. Trussell, M.Y. Chow, "On the use of a lower sampling rate for broken rotor bar detection with DTFT and AR-based spectrum methods", IEEE Transaction on Industrial Electronics, Vol. 55, pp. 1421-1434, 2008.

[17] K.R. Cho, J.H. Lang, S.D. Umans, "Detection of broken rotor bars in induction motors using state and parameter estimation", IEEE Transactions on Industrial Applications, Vol. 28, pp. 702-709, 1992.

[18] İ. Çankaya, F. Vatansever, "Comparison of Fourier and wavelet transforms" (in Turkish), Süleyman Demirel University Journal of Science, Vol. 6, pp. 14-24, 2002.

[19] S.W. Smith, The Scientist and Engineer's Guide to Digital Signal Processing, San Diego, California Technical Publishing, 1997.

[20] S.V. Ustun, M. Demirtas, "Optimal tuning of PI coefficients by using fuzzy-genetic for V/f controlled induction motor", Expert Systems with Applications, Vol. 34, pp. 2714-2720, 2008.

[21] F. Zidani, M.E.H. Benbouzid, D. Diallo, M.S.N. Sait, "Induction motor stator faults diagnosis by a current Concordia pattern-based fuzzy decision system", IEEE Transactions on Energy Conversion, Vol. 18, pp. 469-475, 2003.

[22] R. Bayir, O.F. Bay, "Serial wound starter motor faults diagnosis using artificial neural network", IEEE International Conference on Mechatronics, pp. 194-199, 2004.

[23] R. Bayır, O.F. Bay, "Fault diagnosis in starter motors by classification of wavelet analysis results of faulty starter motor's current signals using fuzzy logic" (in Turkish), Journal of the Faculty of Engineering and Architecture of Gazi University, Vol. 22, pp. 363-374, 2007.

[24] L.A. Pereira, S. Gazzana, "Rotor broken bar detection and diagnosis in induction motors using stator current signature analysis and fuzzy logic", Industrial Electronics Society, Vol. 3, pp. 3019-3024, 2004.

[25] G. Goddu, B. Li, M.Y. Chow, J.C. Hung, "Motor bearing fault diagnosis by fundamental frequency amplitude based fuzzy decision system", 24th Annual Conference of the IEEE, pp. 1961-1965, 1998.

[26] P. Vas, Parameter Estimation, Condition Monitoring, and Diagnosis of Electrical Machines, Oxford, Clarendon Press, 1993.